Published on 07 October 2015. Downloaded by University of Massachusetts - Amherst on 7/21/2022 10:13:25 PM.

Nanoscale

PAPER

View Article Online
View Journal | View Issue

Cite this: *Nanoscale*, 2015, **7**, 18799

Thermal control of ionic transport and fluid flow in nanofluidic channels

Mojtaba Taghipoor,* Arnaud Bertsch and Philippe Renaud

Received 10th August 2015,
Accepted 28th September 2015

DOI: 10.1039/c5nr05409e

www.rsc.org/nanoscale

In this work, we report a nanofluidic gating mechanism that uses the thermal effect for modulating the ionic transport inside nanofluidic channels. The control of the ionic transport inside a nanochannel is demonstrated using electrical conductivity. A thermal gate controls the ionic transport more effectively than most of the other gating mechanisms previously described in the scientific literature. Gating in both bulk and overlapping electric double layer regimes can be obtained. The relatively short response time of opening and closing processes makes it a good candidate for manipulating small molecules in micro- and nanoscale devices.

Controlling the fluidic and ionic transport inside nanochannels is one of the important applications of nanofluidics. Different phenomena were introduced and utilized in nanofluidic channels and pores for controlling the ionic and molecular transport in nanometer scale conduits such as using the electrostatic field effect,[1–3] steric effect[4,5] and liquid reconfiguration.[6,7] Since ions are the only carriers of electric current inside the nanofluidic channels, measuring the electric current across nanochannels has been used as a way to verify the opening or closing of the nanochannels.[1–7]

The ionic mobility of an electrolyte is sensitive to temperature. Consequently, the ionic transport and the electric current in aqueous solutions are dependent on temperature. At the micro and nanoscale, the variation of temperature influences the ionic transport not only by increasing the ionic mobility, but by modifying the channel wall surface properties which also has a significant impact on the ionic and fluidic transport.[8–10] In particular, at the nanoscale, the ionic concentration, pH of the solution and the type and charge of the ions in solution as well as the number of binding sites on the nanochannel wall and equilibrium constants of the surface reactions can influence the temperature sensitivity of the ionic transport inside a nanofluidic channel. According to analytical modeling, the electric conductance of a nanofluidic channel can be increased by about two orders of magnitude by a temperature rise of 65 °C at a low ionic concentration for a silica nanochannel.[10] This modulation factor can provide the possibility of gating in nanoscale fluidic channels.

Microsystems Laboratory, École Polytechnique Fédérale de Lausanne, EPFL STI-IMT-LMIS, Station 17, 1015 Lausanne, Switzerland.
E-mail: mojtaba.taghipoor@epfl.ch

To this aim, the nanofluidic device should have integrated heaters that can increase the nanochannel temperature. Moreover, the response time of the gate to the external stimuli needs to be small enough, so that the channel opening and closing occur on an acceptable time scale, which implies that the heating and cooling processes should be fast. Local heating of the nanochannel can decrease the response time as well as the required heat flux to assess a certain temperature. Joule heating of a thin layer of the metal that is embedded close to the nanochannel or using a plasmonic hot spot[11,12] can appropriately heat up the nanochannel locally.

The local heating will generate a large thermal gradient, which may cause thermophoretic migrations.[11,13] The thermophoretic migration of species inside an electrolyte depends on various factors such as salinity and temperature of the solution, size, charge and hydration shell of the solute as well as the interactions between different solutes.[12,13] The thermophoretic migration of species may cause a reduction or an increase of the electric current inside the nanochannel depending on the direction of migration.

We designed nanofluidic devices that use integrated microheaters in order to control the fluidic transport. The microheater is a 72 μm platinum electrode placed over a 500 nm silicon dioxide layer on top of an array of 40 parallel nanochannels of 110 μm length, 3 μm width and 40 nm height. The fabrication process is detailed in a previous publication.[10] In brief, amorphous silicon was deposited and patterned as a sacrificial layer on a fused silica wafer to shape the nanochannels. This layer was then covered by a 500 nm silicon dioxide layer. The platinum electrodes were then integrated into the device using a normal lift-off technique. Another silicon dioxide layer then insulated the electrodes. The oxide layer was etched so that the amorphous silicon layer became accessible.

Published on 07 October 2015. Downloaded by University of Massachusetts - Amherst on 7/21/2022 10:13:25 PM.

Finally, the amorphous silicon layer was released and the nanochannel became accessible.

Fig. 1a shows a schematic of the nanofluidic device that was mounted on a temperature-controlled mini-cool-plate that kept the external chip temperature at 3 ± 1 °C. A thermally conductive paste was used between the device and the plate in order to enhance the heat transfer. Working at low temperature helps to better illustrate the thermal gating phenomenon by increasing the working temperature range.

The gate is in an off-state when the temperature is low and it turns to an on-state by heating up the micro-heater and the nanochannel. Heating the nanochannel increases the surface charge of the silica nanochannel wall (Fig. 1b). The higher surface charge results in the attraction of a higher number of counter-ions towards the nanochannel. Under these conditions, the ionic flow and the electric conductance will increase.

A relay switch circuit was used to control the on-state pulse time in order to have a unique on-state time in all measurements. Antisymmetric voltages were applied to the gate, so that the gate electric potential of the electrode over the nanochannel region was zero and no electrostatic gating effect appeared inside the nanochannel. Two platinum microelectrodes were placed close to the nanochannel entrance (Fig. 1c) and used in electrical measurements of the nanochannel impedance. The nanochannel resistance was then screened at different gate powers.

Fig. 1d depicts the temperature distribution inside the nanochannel while the 72 μm gate is at 100 °C. The average temperature inside the nanochannel is more than 90 °C while the reference temperature of the whole device is 3 ± 1 °C. This wide temperature range allows a higher level of modulation of the ionic transport. It is worth noting that the nanochannels are connected to large microscale reservoirs that are kept at a low temperature. The values presented in Fig. 1d result from a numerical simulation performed with COMSOL (COMSOL Multiphysics 4.4).

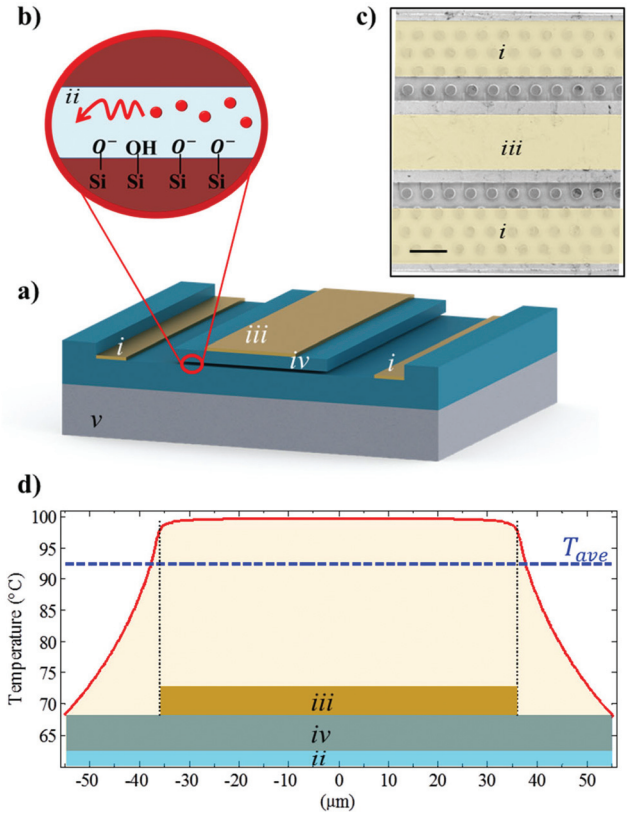

Fig. 1 (a) Schematic of a thermally gated device mounted on a cool plate. The cool plate keeps the temperature at the bottom of the device at 3 ± 1 °C. The impedance of the nanochannel is screened using the integrated platinum electrodes close to the entrance of the nanochannel. *i*: Impedance measurement electrodes. *ii*: Nanochannel. *iii*: Thermal gate. *iv*: Dielectric layer. *v*: Temperature controlled cool plate. (b) Schematic of the ionic transport inside a nanochannel. Heating up the nanochannel enhances the ionic transport by increasing the wall surface charge. (c) Scanning electron micrograph (SEM) of the fabricated device shows the relative position of a thermal gate electrode 72 μm in width and the measurement electrodes. The scale bar is 50 μm. (d) Temperature distribution (red solid line) inside the nanochannel while the gate electrode is at 100 °C. The average temperature (blue dashed line) is about 92 °C.

Results and discussion

The nanochannel was heated up by applying electric DC current to the thermal gate. The resistance of the nanochannel was then measured by applying an AC signal to the measuring electrodes (*i* in Fig. 1) and reading the current. Fig. 2 shows the evolution of the nanochannel resistance and the average temperature at different values of applied power for a 1 mM

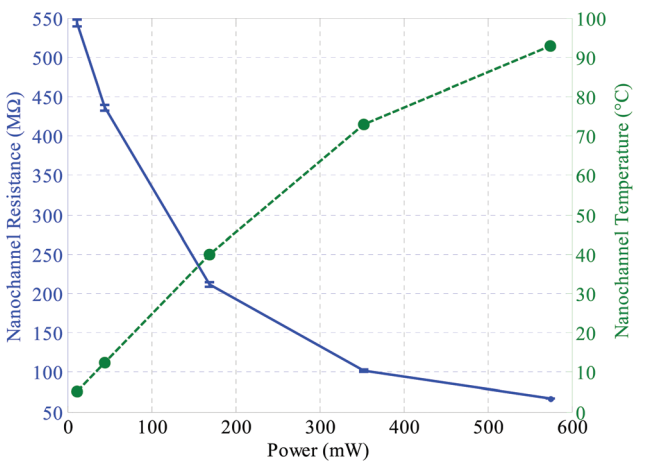

Fig. 2 Evolution of resistance and average temperature of the nanochannel at different applied powers for a 1 mM potassium chloride solution. Increasing the power decreases the nanochannel resistance by heating up the nanochannel. The average temperature is estimated by calibrating the resistance of the nanochannel at 1 M where the change of conductivity is dominated by ion mobilities.[10] The nanochannel length is 110 μm while the width of the gate is only 72 μm.

This journal is © The Royal Society of Chemistry 2015

Published on 07 October 2015. Downloaded by University of Massachusetts - Amherst on 7/21/2022 10:13:25 PM.

potassium chloride solution. Increasing the power decreases the nanochannel resistance. Correlating the power and the achieved electric conductance provides the possibility of controlling the effectiveness of the thermal gate. The values of the power correspond to the proportion of power consumed in the nanochannel region of the gate electrode. The average temperature of the liquid inside the nanochannel was estimated by relating the resistance of the nanochannel at 1 M to temperature, where the change of conductivity is dominated by ionic mobility. In our previous work,[10] we have shown that the temperature dependence of conductivity at a high salt concentration converges to the bulk values which are a = 1.8–2% °C^{-1} for the potassium chloride solution. To this aim, the temperature of the whole device was changed from 2 to 95 °C while it is in contact with a temperature controlled Peltier element. The electrical resistance of the nanochannel was calibrated such that it can be used to estimate the average temperature inside the nanochannel at different applied gate powers for a 1 M solution. The nanochannel conductance measurements are taken after 1 minute in order to wait for thermal equilibrium. The results show that the resistance of the nanochannel at 1 mM is in line with the estimated average temperature. Based on the data from the temperature distribution (Fig. 1d), the temperature of the thermal gate is about 100 °C when a power of 570 mW is applied to the gate (V_{DC} = 8.0 V).

We define the gate effectiveness as the ratio of on- to off-state conductance (G_{on}/G_{off}) in order to compare the performance of the gating methods under different conditions. Fig. 3 depicts the effectiveness of the thermal gate at different ionic concentrations and for deionized water (18 MΩ cm). The thermal gate is able to increase the ionic flux by more than one order of magnitude at low ionic concentrations. As mentioned before, the electrostatic field caused by the wall surface charge influences the ionic transport since the electric double layer (EDL) overlaps at a low ionic concentration. Heating the nanochannel will increase the surface charge density of the silica wall. More ions are attracted toward the nanochannel and its electric conductance increases. Moreover, heating up an aqueous solution increases the ionic mobility by decreasing its viscosity. This occurs for both the bulk and the overlapping EDL regimes. Therefore, a relatively small change in the electric conductance happens at high ionic concentrations. Although the effectiveness is lower at high ionic concentrations, modulating the ionic transport at high ionic concentrations is a clear advantage of the thermal gating method over its electrostatic field effect counterpart. The electrostatic field cannot be used to modulate the ionic transport at high ionic concentrations.

In order to clarify the effect of the wall surface charge, the gating effectiveness of 1 mM potassium chloride solutions at two different pH values has been investigated. As the point of zero charge (PZC) for a silicon dioxide surface is at pH = 3, the surface charge of the nanochannel wall is very low at pH = 4, while a much higher negative charge is expected at pH = 7.[14] Therefore, the dependence of the conductance of the nanochannel on the wall surface charge should be lower at pH = 4. Consequently, at this pH, the sensitivity of the wall surface charge to temperature is low and the increase of the electric conductance can only be related to the bulk effects. Fig. 4 illus-

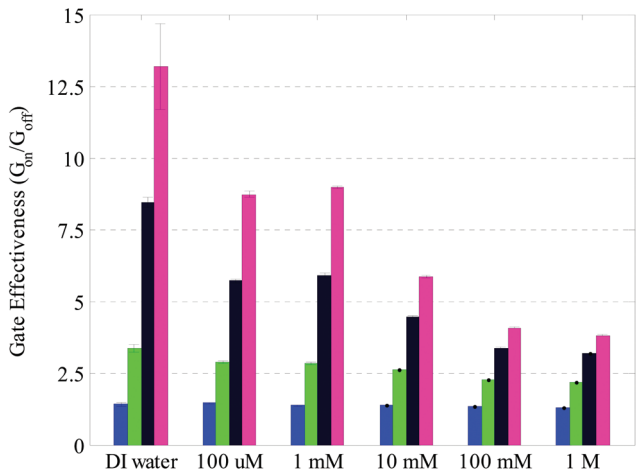

Fig. 3 The gate effectiveness for ΔT = 90 °C (pink), ΔT = 70 °C (black), ΔT = 37 °C (green), ΔT = 10 °C (blue) at different ionic concentrations. The power applied to a 2.5 mm in length gate electrode is 570 mW at ΔT = 90 °C. The gate effectiveness is higher at low ionic concentrations. The nanochannel length is 110 μm while the width of the gate is only 72 μm. The error bars show the 95% confidence interval for 5 measurements.

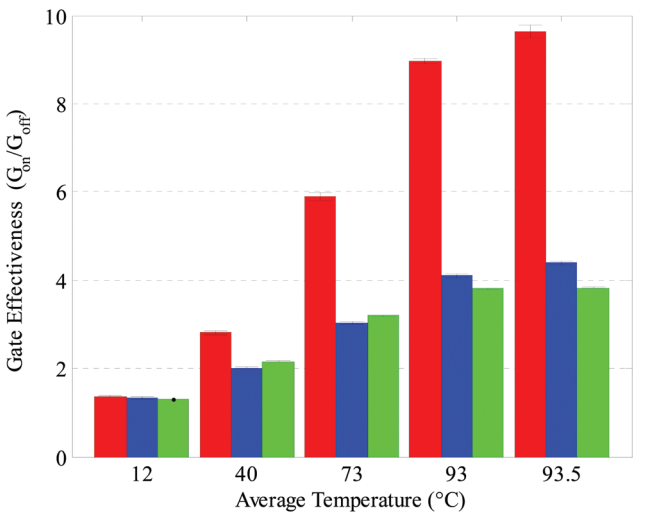

Fig. 4 Effect of the wall surface charge on the gate effectiveness. The figure compares the gate effectiveness for a 1 mM potassium chloride solution at pH = 7 (red) to a solution of the same concentration and pH = 4 (blue) while the solution at 1 M (green) shows the bulk behavior. At pH = 4, the wall surface charge is low and consequently the sensitivity of the conductance of the nanochannel to the temperature is lower. Under these conditions, the increase of the nanochannel conductance is close to the one of the bulk. The nanochannel length is 110 μm while the width of the gate is only 72 μm. The error bars show the 95% confidence interval for 5 measurements.

Published on 07 October 2015. Downloaded by University of Massachusetts - Amherst on 7/21/2022 10:13:25 PM.

trates the contribution of the enhancement of the surface charge effect due to the temperature increase for both solutions. A 1 M potassium chloride solution is used as a bulk control to demonstrate the ionic mobility dependence of the electric conductance only on the temperature. As shown in Fig. 4, the gate effectiveness of the solution at pH = 4 is close to the bulk while there is a major increase at pH = 7. This difference emphasizes that the effectiveness of the thermal gate is mainly caused by the unique nanofluidic effect due to the charged wall. However, the effectiveness at the bulk regime is still comparable to the ones of other gating methods. The complete theory was discussed in our previous work.[10]

Table 1 represents the values of the reported gate effectiveness for various nanofluidic transport gates. The reported values are the maximum achieved performances in the mentioned publications. For the case of the electrostatic gating, the ratio of maximum to minimum electric conductance is defined as the gate effectiveness. According to the table, the gate effectiveness is less than 5 for most of the cases. A small value of the gate effectiveness implies that the ionic transport can neither be stopped completely nor be enhanced considerably. Although the introduced gating methods are successful in modulating the ionic transport, they are still far from ideally opening and closing the nanochannel.

Some of the gating methods are limited by technological restrictions. For example, the effectiveness of the field effect gates is limited by the breakdown of the dielectric layer. Additionally, having the gate electrode only on one side of the nanochannel wall decreases the effectiveness of the field effect gate in a nanochannel platform[2] while the gate effectiveness of a similar gate electrode surrounded nanotube is doubled.[3]

Table 1 Reported gate effectiveness for different types of gating mechanisms. The values are mostly less than one order of magnitude

Article	Category	Gating stimulus	Gate effectiveness[a]
Xia *et al.*[5]	Steric	pH	10
Hou *et al.*[15]	Steric	Potassium ion	1.3
Yameen *et al.*[4]	Steric	Temperature	3.4
Yameen *et al.*[16]	Steric	pH	4
Tian *et al.*[17]	Steric	Zinc ion	1.3
Tian *et al.*[18]	Steric	Mercury	3.2
Liu *et al.*[19]	Steric	pH and/or potassium ion	2.3
Fan *et al.*[3]	Field effect	Gate voltage	2.9
Karnik *et al.*[2]	Field effect	Gate voltage	1.3
Schoch and Renaud[1]	Field effect	Gate voltage	1.6
Nam *et al.*[20]	Field effect	Gate voltage	9
Joshi *et al.*[21]	Field effect	Gate voltage	2.6
Jiang and Stein[22]	Field effect	Gate voltage	1.2

[a] Gate effectiveness is defined as the ratio of on- to off-state conductance. For the case of the field effect, the maximum and minimum achieved conductance is considered as the open- and closed-state, respectively.

The effectiveness of the thermal gating method exceeds one order of magnitude at low ionic concentrations while other gating methods have considerably lower effectiveness. Heating the nanochannel does not need a complicated microfabrication process. Moreover, the thermal gate does not suffer from the limitations in device manufacturing such as dielectric breakdown limitations for the field effect gating method. However, the thermal effect used in thermal gating may limit the choice of molecules used in such a system to the ones that can withstand the local temperature reached inside the nanochannel. Depending on the local temperature reached during thermal gating some biomolecules such as proteins may be detrimental.

Thermal gating can be fast. Its response time is determined, on the one hand, by the thermal diffusivity of the materials, which determines the dynamical temperature profile, and on the other hand, by the ion diffusion and the reaction rate of surface reactions, which determine the dynamical ion concentration profile in the case of change of surface charge. In Fig. 5, some examples of the applied thermal pulses are depicted. 200 ms pulses (left side of Fig. 5a) have higher effectiveness than 50 ms pulses (right side). Fig. 5b shows the opening and closing process of a single 200 ms pulse. The closing process needs more time than the opening one. In our particular design, the typical closing time is about $\tau_c \cong 400$ ms whereas the opening is much faster. The closing time is indicated by τ_c in the figure. As depicted in Fig. 5c, for longer pulses, we clearly see the thermal time constant in both opening and closing transitions.

The pulses in Fig. 5a–c correspond to a 1 M ionic concentration, which we consider as bulk regime ionic transport. Therefore, the result can represent the average temperature inside the nanochannel at any ionic concentration using the calibration that was performed before (see Fig. 2). Alternatively, it can represent the proportion of the ionic mobility in the enhancement of the ionic transport. At lower ionic concentrations, the additional effect of the surface charge appears.

Fig. 5d depicts 5 s pulses at different ionic concentrations. First, it emphasizes the additional increase of the gate effectiveness at low ionic concentrations that occurs only in the EDL overlapping regime. Secondly, it shows that the gating dynamics at low ionic concentrations is different from the bulk regime. As represented in Fig. 5d, the electric conductance does not settle down instantly to its off-state value. By switching the gate off, the electric conductance decreases to a value higher than the normal off-state. This decrease occurs in a time in the order of τ_c. Then, it decreases to the normal value of the off-state with a slower rate. Thus, the slower rate of settling down cannot be justified by the temperature. Besides, this effect appears only at low ionic concentrations where the nanofluidic regime occurs. In other words, it is dependent on the surface charge of the nanochannel.

This journal is © The Royal Society of Chemistry 2015

Published on 07 October 2015. Downloaded by University of Massachusetts - Amherst on 7/21/2022 10:13:25 PM.

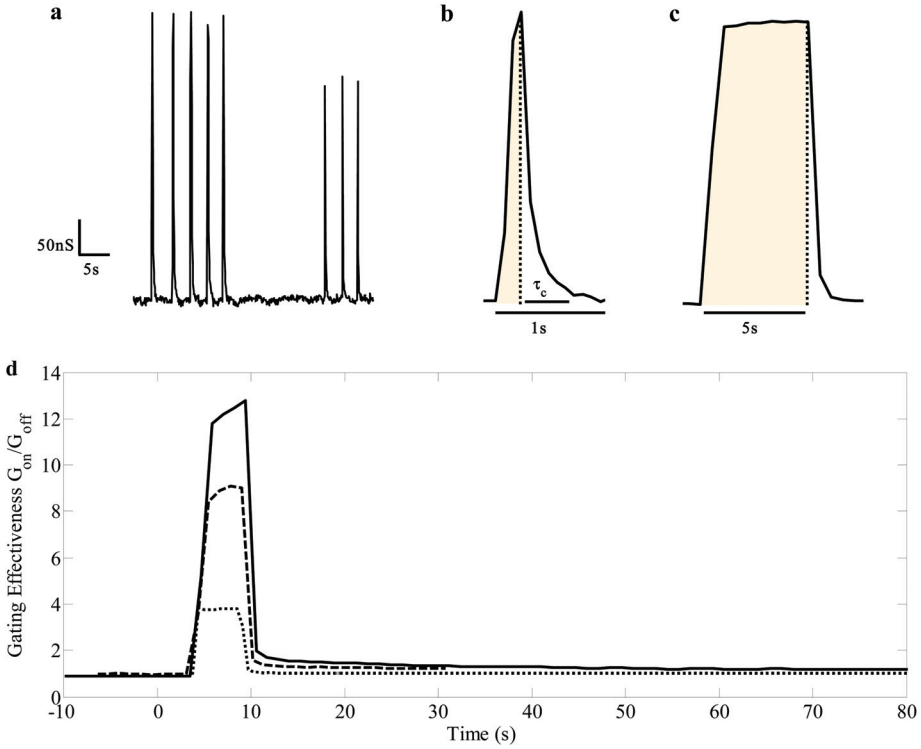

Fig. 5 (a) Short time pulses can be applied for thermal gating. The signal shows five 200 ms (left) and three 50 ms (right) on-state pulses at 1 M ionic concentration. (b) A zoomed view of a 200 ms pulse. Both opening and closing occur in a relatively short period of time. (c) A single 5 s pulse. The closing process is still quick, even if the gate is kept open for a longer time. (d) Comparison of 5 s pulses at 1 M (dotted line), 1 mM (dashed line) ionic concentrations and DI water (solid line). The vertical axis shows the ratio of on- to off-state conductance. At low ionic concentration, the conductance needs excess time to stabilize which results from the dynamical ion concentration profile.

Conclusion

We demonstrated the possibility of controlling the ionic transport in nanochannels using thermal gating for the first time. A thermal gate modulates the ionic transport by heating up the nanochannel. It increases the ionic transport *via* raising both the ionic mobility and the surface charge of the nanochannel wall. The surface charge of a silica nanochannel wall increases with temperature. The higher temperature of the nanochannel changes the equilibrium constant of the reactions at the surface such that a higher number of negatively charged sites are present on the surface. This results in an additional electrostatic effect that does not occur in bulk regimes. The dependency of the ionic transport on temperature in bulk regimes is attributed only to the increased ionic mobility with temperature.

According to the two mentioned mechanisms, the effectiveness of the thermal gating is dependent on the ionic concentration. At low ionic concentrations, a high effectiveness is achieved while it decreases by increasing the ionic concentration. In contrast to the field effect gating method, the thermal gating can still modulate the ionic transport at bulk regimes.

The thermal gate effectiveness was compared to other gating mechanisms. The thermal gate has a higher effectiveness and requires less technological restrictions compared to other gating mechanisms.

The thermal gate is fast enough to be used for the manipulation of small molecules inside nanofluidic channels. A response time in the order of tens of milliseconds was observed for the opening process. The closing process needs hundreds of milliseconds at the maximum achieved effectiveness.

The thermal gate can be used in applications that require controlling the ionic or fluidic transport at the small scale. The thermal gate has the possibility of being stimulated remotely, which is an advantage over the field effect gating method. It can remotely control the delivery process of sub-femtoliter volumes.

Acknowledgements

The authors acknowledge valuable support from CMI (Center of MicroNanoTechnology) for microfabrication processes. The authors would also like to thank Mr Harald Van Lintel for helpful technical assistance. This work was partially funded by MSRT under grant number MSRT-89100219.

References

1 R. B. Schoch and P. Renaud, *Appl. Phys. Lett.*, 2005, **86**, 253111.

Published on 07 October 2015. Downloaded by University of Massachusetts - Amherst on 7/21/2022 10:13:25 PM.

2 R. Karnik, R. Fan, M. Yue, D. Y. Li, P. D. Yang and A. Majumdar, *Nano Lett.*, 2005, **5**, 943–948.
3 R. Fan, M. Yue, R. Karnik, A. Majumdar and P. Yang, *Phys. Rev. Lett.*, 2005, **95**, 086607.
4 B. Yameen, M. Ali, R. Neumann, W. Ensinger, W. Knoll and O. Azzaroni, *Small*, 2009, **5**, 1287–1291.
5 F. Xia, W. Guo, Y. Mao, X. Hou, J. Xue, H. Xia, L. Wang, Y. Song, H. Ji, Q. Ouyang, Y. Wang and L. Jiang, *J. Am. Chem. Soc.*, 2008, **130**, 8345–8350.
6 M. R. Powell, L. Cleary, M. Davenport, K. J. Shea and Z. S. Siwy, *Nat. Nanotechnol.*, 2011, **6**, 798–802.
7 S. N. Smirnov, I. V. Vlassiouk and N. V. Lavrik, *ACS Nano*, 2011, **5**, 7453–7461.
8 J.-P. Hsu, Y.-H. Tai, L.-H. Yeh and S. Tseng, *Langmuir*, 2012, **28**, 1013–1019.
9 R. Venditti, X. Xuan and D. Li, *Microfluid. Nanofluid.*, 2006, **2**, 493–499.
10 M. Taghipoor, A. Bertsch and P. Renaud, *ACS Nano*, 2015, **9**, 4563–4571.
11 F. Nicoli, D. Verschueren, M. Klein, C. Dekker and M. P. Jonsson, *Nano Lett.*, 2014, **14**, 6917–6925.
12 M. Braun and F. Cichos, *ACS Nano*, 2013, **7**, 11200–11208.
13 M. Belkin, S.-H. Chao, G. Giannetti and A. Aksimentiev, *J. Comput. Electron.*, 2014, **13**, 826–838.
14 M. Taghipoor, A. Bertsch and P. Renaud, *Phys. Chem. Chem. Phys.*, 2015, **17**, 4160–4167.
15 X. Hou, W. Guo, F. Xia, F.-Q. Nie, H. Dong, Y. Tian, L. Wen, L. Wang, L. Cao, Y. Yang, J. Xue, Y. Song, Y. Wang, D. Liu and L. Jiang, *J. Am. Chem. Soc.*, 2009, **131**, 7800–7805.
16 B. Yameen, M. Ali, R. Neumann, W. Ensinger, W. Knoll and O. Azzaroni, *J. Am. Chem. Soc.*, 2009, **131**, 2070–2071.
17 Y. Tian, X. Hou, L. Wen, W. Guo, Y. Song, H. Sun, Y. Wang, L. Jiang and D. Zhu, *Chem. Commun.*, 2010, **46**, 1682–1684.
18 Y. Tian, Z. Zhang, L. Wen, J. Ma, Y. Zhang, W. Liu, J. Zhai and L. Jiang, *Chem. Commun.*, 2013, **49**, 10679–10681.
19 M. Liu, H. Zhang, K. Li, L. Heng, S. Wang, Y. Tian and L. Jiang, *Adv. Funct. Mater.*, 2015, **25**, 421–426.
20 S.-W. Nam, M. J. Rooks, K.-B. Kim and S. M. Rossnagel, *Nano Lett.*, 2009, **9**, 2044–2048.
21 P. Joshi, A. Smolyanitsky, L. Petrossian, M. Goryll, M. Saraniti and T. J. Thornton, *J. Appl. Phys.*, 2010, 107.
22 Z. Jiang and D. Stein, *Phys. Rev. E: Stat. Phys., Plasmas, Fluids, Relat. Interdiscip. Top.*, 2011, 83.

This journal is © The Royal Society of Chemistry 2015